Proton Structure and Prediction of pp Elastic Scattering at LHC at Center-of-Mass Energy 7 TeV

M. M. Islam[1], J. Kašpar[2,3], R. J. Luddy[1]

[1]Department of Physics, University of Connecticut, Storrs, CT 06269 USA
[2]Institute of Physics of the Academy of Sciences of the Czech Republic, Prague, Czech Republic
[3]CERN 1211 Geneva 23, Switzerland

Talk presented by M. M. Islam

Abstract

Our phenomenological investigation of high-energy pp and $\bar{p}p$ elastic scattering and study of low-energy models of nucleon structure have led us to a physical picture of the proton; namely, the proton is a $q\bar{q}$-condensate enclosed chiral bag. Based on this picture, we predict the pp elastic differential cross section at LHC at c.m. energy 7 TeV. Experimental measurement of pp elastic $d\sigma/dt$ at LHC by the TOTEM Collaboration from $|t| = 0$ to $|t| = 10$ GeV^2 will test our model of proton structure. We also compare our prediction of $d\sigma/dt$ with the predictions of the Block et al. model and the BSW (Bourrely, Soffer, Wu) model.

1. Introduction

Let me start by saying that a physical picture of the proton has emerged from our phenomenological investigation of high energy pp and $\bar{p}p$ elastic scattering measurements and our study of various non-perturbative models of nucleon structure. The physical picture is that the proton is comprised of three regions: an outer cloud of $q\bar{q}$ condensed ground state of size 0.86 F, an intermediate shell of baryonic charge of size 0.44 F, and a core of size 0.2 F, where valence quarks are confined (Fig. 1) [1].

The high energy elastic pp and $\bar{p}p$ measurements were done beginning with the advent of the CERN pp collider in the early seventies, then continuing with the CERN SPS Collider in the eighties, and ending in the mid-nineties with the Tevatron measurement of $\bar{p}p$ elastic scattering at 1.8 TeV c.m. energy. During this same period, various theoretical groups devoted enormous effort to develop non-perturbative models of nucleon structure based on low-energy properties of the nucleon; for example, Skyrmion model, MIT bag model, Little Bag model, topological soliton model, Chiral bag model etc. [2]

Our finding is that the proton is described by an effective field theory model: A gauged Gell-Mann-Levy linear σ-model with vector mesons ρ and ω introduced as gauge bosons. The model gives rise to an effective action known as Wess-Zumino-Witten (WZW) action and leads to an interactive Dirac sea of quarks and antiquarks forming the outer region of the proton.

Currently, pp elastic scattering at c.m. energy 7 TeV is planned to be measured at the Large Hadron Collider (LHC) by the TOTEM (Total, Elastic and Diffractive Scattering

Measurement) Collaboration over a large momentum transfer range: $|t|\sim 10^{-3}$ to $|t| > 10$ GeV^2. We present our prediction of pp elastic $d\sigma/dt$ at c.m. energy 7 TeV in the range $|t| = 0 - 10$ GeV^2 and compare our results with those of the Block et al. model and the Bourrely, Soffer, Wu model. Precise measurement of $d\sigma/dt$ by the TOTEM Collaboration will determine how well our prediction holds up and provide a test of our model.

2. Linear σ-Model and Hidden Gauge Symmetry

We begin with the Gell-Mann-Levy linear σ-model which has $SU(2)_{\mathrm{L}} \times SU(2)_{\mathrm{R}}$ global symmetry and spontaneous breakdown of chiral symmetry. The model is given by the Lagrangian density

$$\mathcal{L} = \bar{\psi}\, i\, \gamma^{\mu}\partial_{\mu}\psi + \tfrac{1}{2}\left(\partial_{\mu}\sigma\, \partial^{\mu}\sigma + \partial_{\mu}\vec{\pi}\, \partial^{\mu}\vec{\pi}\right) - G\bar{\psi}[\sigma + i\, \vec{\tau}\cdot\vec{\pi}\, \gamma^{5}]\psi - \lambda(\sigma^2 + \vec{\pi}^2 - f_{\pi}^2)^2. \quad (1)$$

In our study, the fermions are identified with quarks, and we begin with a two flavor model for quarks (u and d). We introduce a scalar-isoscalar field $\zeta(x)$ and a unitary field $U(x)$ in the following way:

$$\sigma(x) + i\, \vec{\tau}\cdot\vec{\pi}(x) = \zeta(x)U(x). \quad (2)$$

$\zeta(x)$ is the magnitude of the fields $\sigma(x)$ and $\vec{\pi}(x)$: $\zeta(x) = \sqrt{\sigma^2(x) + \vec{\pi}^2(x)}$. Using right and left fermion fields:

$$\psi_{\mathrm{R}}(x) = \tfrac{1}{2}(1 + \gamma^5)\, \psi(x), \quad \psi_{\mathrm{L}}(x) = \tfrac{1}{2}(1 - \gamma^5)\, \psi(x), \quad (3)$$

the Lagrangian density (Eq.1) can now be written as:

$$\mathcal{L} = \bar{\psi}_{\mathrm{R}}\, i\, \gamma_{\mu}\, \partial_{\mu}\psi_{\mathrm{R}} + \bar{\psi}_{\mathrm{L}}\, i\, \gamma^{\mu}\, \partial_{\mu}\psi_{\mathrm{L}} + \tfrac{1}{2}\partial_{\mu}\zeta\, \partial^{\mu}\zeta + \tfrac{1}{4}\zeta^2 tr\left[\partial_{\mu}U\, \partial^{\mu}U^{\dagger}\right]$$
$$-G\, \zeta\, [\bar{\psi}_{\mathrm{L}}U\, \psi_{\mathrm{R}} + \bar{\psi}_{\mathrm{R}}\, U^{\dagger}\, \psi_{\mathrm{L}}] - \lambda(\zeta^2 - f_{\pi}^2)^2. \quad (4)$$

Under global right and left transformations

$$\psi_{\mathrm{R}}(x) \to R\, \psi_{\mathrm{R}}(x), \;\; \psi_{\mathrm{L}}(x) \to L\, \psi_{\mathrm{L}}(x) \quad (5a)$$
$$U(x) \to L\, U(x)\, R^{\dagger}, \;\; \zeta(x) \to \zeta(x), \quad (5b)$$

and the Lagrangian density (Eq. 4) is manifestly invariant under these global transformations. If we now consider chiral symmetry ($\psi \to e^{\theta\gamma^5}\psi$), then

$$\psi_{\mathrm{R}}(x) \to e^{\theta}\psi_{\mathrm{R}}(x), \qquad \psi_{\mathrm{L}}(x) \to e^{-\theta}\psi_{\mathrm{L}}(x) \quad (6a)$$
$$U(x) \to\; e^{-\theta}U(x)e^{-\theta}, \quad \zeta(x) \to \zeta(x) \quad (6b)$$

where $\theta = -i\, T^a\, \theta^a$ ($T^a = \frac{1}{2}\tau^a$) and θ^a's are global.

The potential energy density $v(\zeta) = \lambda\, (\zeta^2 - f_{\pi}^2)^2$ in Eq. 1 vanishes when $\zeta(x) = f_{\pi}$. This corresponds to the ground state (lowest energy state) of the system. Let us consider a ground state configuration

$$\sigma_0(x) + i\, \vec{\tau}\, \cdot\vec{\pi}_0(x) = \zeta_0\, U(x), \qquad (\zeta_0 = f_{\pi}). \quad (7)$$

Under a chiral transformation,

$$\zeta_0\, U(x) \to \zeta_0\, U'(x) = \zeta_0\, e^{-\theta}\, U(x)\, e^{-\theta}. \tag{8}$$

This also corresponds to a ground state, because $\zeta_0 = f_\pi$ and $v(\zeta) = 0$, but with a different field configuration $\zeta_0 U'(x)$. We find that under a global chiral transformation – while the Lagrangian remains invariant, the ground state changes. In fact, we can generate an infinite number of ground states using the continuous chiral transformation. This represents the spontaneous breakdown of the global chiral symmetry. Writing $U(x) = \exp[i\, \vec{\tau}\, \cdot \frac{\vec{\varphi}(x)}{f_\pi}]$, we can identify $\vec{\varphi}(x)$ as the isovector pion field, f_π as the pion decay coupling constant ($f_\pi \simeq 93$ MeV), and the pions as Goldstone bosons. When $\zeta(x)$ is replaced by its vacuum value f_π, the Lagrangian (4) corresponds to a nonlinear σ-model.

Following Bando et al.[3], we now introduce the idea of a hidden local symmetry. Bando et al. took the symmetry to be $[SU(2)]_{\text{hidden}}$. We consider an extended version of this approach, and following Meissner et al.[4] take the symmetry to be $[SU(2) \times U(1)]_{\text{hidden}}$. To implement the idea of a hidden local symmetry, one writes $U(x) = \xi_{\text{L}}^{\dagger}(x)\xi_{\text{R}}(x)$, where $\xi_{\text{L}}(x)$ and $\xi_{\text{R}}(x)$ are $SU(2)$ -valued fields which transform in the following way under $[SU(2)_{\text{L}} \times SU(2)_{\text{R}}]_{\text{global}} \times [SU(2) \times U(1)]_{\text{local}}$:

$$\xi_{\text{R}}(x) \to h(x)\, \xi_{\text{R}}(x) R^{\dagger}, \qquad \xi_{\text{L}}(x) \to h(x)\, \xi_{\text{L}}(x) L^{\dagger}, \tag{9}$$

where $h(x) \in [SU(2) \times U(1)]_{\text{local}}$. Therefore,

$$U(x) = \xi_{\text{L}}^{\dagger}(x)\, \xi_{\text{R}}(x) \to L\, U(x) R^{\dagger} \tag{10}$$

as required by the global symmetry of the Lagrangian (4).

Let us focus on the unitary (or pion) sector of the Lagrangian (4):

$$\begin{aligned} \mathcal{L}_U &= \tfrac{1}{4}\zeta^2\, tr\left[\partial_\mu U\, \partial^\mu U^{\dagger}\right] \\ &= -\tfrac{1}{4}\zeta^2\, tr\left[\partial_\mu \xi_{\text{L}}\, \xi_{\text{L}}^{\dagger} - \partial_\mu \xi_{\text{R}}\, \xi_{\text{R}}^{\dagger}\right]^2 \end{aligned} \tag{11}$$

We gauge this symmetry by introducing the vector mesons ρ and ω as gauge bosons of the $[SU(2) \times U(1)]_{\text{hidden}}$ symmetry. Gauging is done easily by replacing the ordinary derivative by the covariant derivative: $\partial_\mu \to D_\mu = \partial_\mu + \mathcal{V}_\mu$, where

$$\mathcal{V}_\mu = -\tfrac{i}{2}\, g[\vec{\tau} \cdot \vec{\rho}_\mu + \omega_\mu] \tag{12}$$

and $\mathcal{V}_\mu$ transforms under the hidden symmetry in the following way:

$$\mathcal{V}_\mu \to h\, \mathcal{V}_\mu\, h^{\dagger} + h\, \partial_\mu\, h^{\dagger}. \tag{13}$$

The Lagrangian density of the gauged hidden-symmetry model is taken as

$$\begin{aligned} \mathcal{L}_U = &-\tfrac{1}{4}\zeta^2 tr[(D_\mu\, \xi_{\text{L}})\xi_{\text{L}}^{\dagger} - (D_\mu \xi_{\text{R}})\xi_{\text{R}}^{\dagger}]^2 \\ &-\tfrac{1}{2}\zeta^2 tr\left[(D_\mu\, \xi_{\text{L}})\xi_{\text{L}}^{\dagger} + (D_\mu \xi_{\text{R}})\xi_{\text{R}}^{\dagger}\right]^2 + \frac{1}{2g^2} tr[F_{\mu\nu}F^{\mu\nu}], \end{aligned} \tag{14}$$

where the first term is exactly the same as the original term $\frac{1}{4}\zeta^2\ tr[\partial_\mu U\ \partial^\mu U^\dagger\ ]$. The second term is a gauge invariant term that generates the masses of the vector mesons. The third term is the Lagrangian density of the gauge field $\mathcal{V}_\mu(x)$, where $F_{\mu\nu}$ is the nonabelian field tensor: $F_{\mu\nu} = \partial_\mu \mathcal{V}_\nu\ - \partial_\nu \mathcal{V}_\mu + [\mathcal{V}_\mu, \mathcal{V}_\nu]$. This term provides the fourth order derivative term in the Skyrme model [5].

The gauge field $\mathcal{V}_\mu(x)$ of the hidden gauge symmetry leads to a left gauge field $A_\mu^{\mathrm{L}}(x)$ and a right gauge field $A_\mu^{\mathrm{R}}(x)$ associated with local left and local right chiral transformations [6]. This allows us to write the Lagrangian density in the quark sector in a chirally invariant form, i.e., invariant under local chiral transformations: $\psi_{\mathrm{R}}(x) \to R(x)\ \psi_{\mathrm{R}}(x)$, $\psi_{\mathrm{L}}(x) \to L(x)\ \psi_{\mathrm{L}}(x)$, $U(x) = \zeta_{\mathrm{L}}^\dagger(x)\ \zeta_{\mathrm{R}}(x)\ \to L(x)\ \zeta_{\mathrm{L}}^\dagger(x)\ \zeta_{\mathrm{R}}(x)\ R^\dagger(x) = L(x)U(x)\ R^\dagger(x)$. We find [6]

$$\mathcal{L}_{\mathrm{q}} = \bar{\psi}_{\mathrm{L}}\ i\ \gamma^\mu\big(\partial_\mu + A_\mu^{\mathrm{L}}\big)\psi_{\mathrm{L}} + \bar{\psi}_{\mathrm{R}}(x)\ i\ \gamma^\mu\big(\partial_\mu + A_\mu^{\mathrm{R}}\big)\psi_{\mathrm{R}} - G\ \zeta\ [\bar{\psi}_{\mathrm{L}}\ U\ \psi_{\mathrm{R}} + \bar{\psi}_{\mathrm{R}}\ U^\dagger\ \psi_{\mathrm{L}}]. \qquad (15)$$

3. Wess-Zumino-Witten (WZW) Action and Topological Soliton of the Nonlinear σ-Model

At this point, a new aspect of the model appears, which can be seen by writing the model in path integral formalism and recognizing that the fermion measure is gauge dependent. To this end, we consider a three flavor model for quarks (u, d, s), so that the symmetry group is local $SU(3)_{\mathrm{L}}\ \times SU(3)_{\mathrm{R}}$. The gauge dependent fermion measure can be written as a gauge independent fermion measure multiplied by a Jacobian:

$$\int d\psi\ \ d\psi^\dagger = e^{i\,\Gamma[U,\mathcal{V}]}\ \int\ d\psi^0\ d\psi^{0\,\dagger}, \qquad (16)$$

where the Jacobian has been expressed in the form $\exp(i\,\Gamma[U,\mathcal{V}])$ and $\Gamma[U,\mathcal{V}]$ can be identified as the Wess-Zumino-Witten (WZW) action. Here $\psi_{\mathrm{L}}^0(x) = \xi_{\mathrm{L}}(x)\psi_{\mathrm{L}}(x)$, $\psi_{\mathrm{R}}^0(x) = \xi_{\mathrm{R}}(x)\psi_{\mathrm{R}}(x)$; therefore, $\psi_{\mathrm{L}}^0(x)$ and $\psi_{\mathrm{R}}^0(x)$ transform only under the hidden symmetry. We can now write down the action functional or effective action of the model in the following way:

$$e^{i\,W[U,\zeta,\mathcal{V},\psi,\psi^\dagger]} = \frac{1}{\mathcal{N}}\int dU\ d\zeta\ d\psi^0\ d\psi^{0\,\dagger}\ \cdot\ e^{i\,\Gamma_{WZW}[U,\mathcal{V}]+i\,S[U,\zeta,\mathcal{V}]+i\,S[\zeta,\psi^0,\psi^{0\,\dagger},\mathcal{V}]}. \qquad (17)$$

Here $S[U,\zeta,\mathcal{V}]$ is the action in the unitary field U sector (or, pion sector):

$$S[U,\zeta,\mathcal{V}] = \int d^4x\ \mathcal{L}_U(U,\zeta,\mathcal{V}) \qquad (18)$$

with $\mathcal{L}_U$ given by Eq. (14) and expressed in the unitary gauge: $\xi_{\mathrm{L}}^\dagger(x) = \xi_{\mathrm{R}}(x) = \xi(x), U(x) = \xi^2(x)$. $S[\zeta,\psi^0,\psi^{0\,\dagger},\mathcal{V}]$ is the action in the quark-scalar sector[6]:

$$S\left[\zeta,\psi^0,\psi^{0\,\dagger},\mathcal{V}\right] = \int d^4x\ [\bar{\psi}^0\ i\ \gamma^\mu\big(\partial_\mu + \mathcal{V}_\mu\big)\psi^0 + \tfrac{1}{2}\ \partial_\mu\zeta\ \partial^\mu\zeta - G\ \zeta\ \bar{\psi}^0\psi^0 - \lambda(\zeta^2 - f_\pi^2)^2]. \qquad (19)$$

We note that $\psi^0(x) = \psi_{\mathrm{L}}^0(x) + \psi_{\mathrm{R}}^0(x)$ transforms only under the hidden symmetry: $\psi^0(x) \to h(x)\ \psi^0(x)$. In Eq. (17), $\mathcal{V}_\mu(x)$ is treated as an external gauge field, and $\mathcal{N}$ is an appropriate normalization constant.

If we consider the approximation that the scalar field $\zeta(x)$ can be replaced by its ground state value f_π in the pion sector, then from Eq. (17) we obtain

$$e^{iW[U,\zeta,\mathcal{V},\psi,\psi^\dagger]} \simeq \frac{1}{\mathcal{N}} \int dU\, e^{i\Gamma_{WZW}[U,\mathcal{V}]+iS[U,f_\pi,\mathcal{V}]} \int d\zeta\, d\psi^0\, d{\psi^0}^\dagger e^{iS[\zeta,\psi^0,{\psi^0}^\dagger,\mathcal{V}]} \quad (20)$$

where

$$S[U,f_\pi,\mathcal{V}] = \int d^4x \left\{\frac{1}{4} f_\pi^2\, tr\left[\partial_\mu U\, \partial^\mu U^\dagger\right] - \frac{1}{2} f_\pi^2 tr\left[(D_\mu \xi^\dagger)\xi + (D_\mu \xi)\xi^\dagger\right]^2 + \frac{1}{2g^2}\, tr[F_{\mu\nu}F^{\mu\nu}]\right\}. \quad (21)$$

The combined action

$$\Gamma_{WZW}[U,\mathcal{V}] + S[U,f_\pi,\mathcal{V}] \quad (22)$$

describes the topological soliton of the nonlinear σ-model (NLσM).

We note that the Wess-Zumino-Witten action in its simplest approximation can be written as $\Gamma_{WZW}[U,\mathcal{V}] = \int d^4x\, \mathcal{L}_{WZW}$, where $\mathcal{L}_{WZW} = g_\omega \omega_\mu B^\mu$ [7]; B^μ is the conserved baryonic current

$$B^\mu = \frac{1}{24\pi^2} \epsilon^{\mu\nu\rho\sigma}\, tr[U^\dagger\, \partial_\nu U\, U^\dagger \partial_\rho U U^\dagger \partial_\sigma U], \quad (23)$$

and $U(x) = \exp[i\, \vec{\tau} \cdot \frac{\vec{\varphi}(x)}{f_\pi}]$. $\mathcal{L}_{WZW}$ shows that the vector meson ω couples to the baryonic current just like a gauge boson and the baryonic current is topological (geometrical) in the nonlinear σ-model.

4. Quark-Scalar Sector of Linear σ-Model and Emergence of Condensate Enclosed Chiral Bag Model

Eq. (19) shows that we have a quark-scalar sector described by the action $S[\zeta, \psi^0 {\psi^0}^\dagger, \mathcal{V}]$, which is not present in the NLσM. In the NLσM, the scalar field $\zeta(x)$ is replaced by its vacuum value f_π from the very beginning; so the scalar degree of freedom never appears in this model. Also, it is implicitly assumed that once the WZW action (originating from the gauge dependence of the fermion measure) is taken into account in addition to the action $S[U,f_\pi,\mathcal{V}]$, no further interactions of quarks and antiquarks need to be considered. In particular, this means the action in the quark-scalar sector (Eq. (19)) reduces to

$$S\left[\psi^0, {\psi^0}^\dagger\right] = \int d^4x\, \bar{\psi}^0\ i\, \gamma^\mu \partial_\mu \psi^0. \quad (24)$$

So, what is left from this sector is a non-interacting Dirac sea of massless quarks and antiquarks.

Our investigation, however, shows that the quark-scalar sector (Eq. (19)) can provide ground state energy significantly lower than the energy of the non-interacting Dirac sea. We find that the ground state energy of the interacting system minus the ground state energy of the non-interacting system is given by [8]

$$\Delta E = \int d^3x \left[-\frac{1}{2}\left(\vec{\nabla}\zeta\right)^2 + v(\zeta) + 4\,\lambda\,\zeta^2\left({f_\pi}^2 - \zeta^2\right)\right] + E_{\mathrm{g}}^{KE}, \quad (25)$$

where the scalar field is taken to be time-independent; $v(\zeta)$ is the potential energy density: $v(\zeta) = \lambda\,(\zeta^2 - f_\pi^2)^2$, and $E_{\rm g}^{KE}$ is the kinetic energy of the interacting quarks and antiquarks in the Dirac sea. Eq. (25) shows that if the scalar field $\zeta(r)$ falls sharply from its pion sector value f_π to zero at some critical distance $r = r_{\rm c}$ (as shown in Fig. 2), then the term $-\frac{1}{2}\int d^3x\,\left(\vec{\nabla}\zeta\right)^2$ can be very large and lower the total energy of the system by a significant amount. In fact, if we take a ζ-field given by $f_\pi\,\theta(r - r_{\rm c})$, then the first term on the right-hand-side of Eq. (25) leads to a large surface energy: $-\frac{1}{2}\,f_\pi^2\,4\,\pi\,r_{\rm c}^2\,\delta(0)$, which is infinitely negative. What this means is that for a $\zeta(r)$ falling sharply from $\zeta(r) = f_\pi$ to $\zeta(r) = 0$, the mass of the soliton will be reduced by a large amount, which can be as large as ~600 MeV. It resolves a major problem of the NLσM, which has been very successful in describing the low energy properties of the nucleon as a topological soliton, but has always obtained a large mass for the soliton, typically 1600 MeV as compared to the nucleon mass 939 MeV (even when the model is extended to include the chiral partners a_1 and f_1 mesons of ρ and ω [9].

There are several implications of the above behavior of the scalar field. As the topological baryonic charge now occupies only the region $r_{\rm c} < r \lesssim r_{\rm B}$, where $r_{\rm B}$ is the root-mean-square radius of baryonic charge distribution, there have to be valence quarks in the core to make up for the total baryonic charge 1 (Fig. 2). Assuming $\zeta(r)$ drops from f_π to zero as $f_\pi\,\theta(r - r_{\rm c})$, we end up with a model of nucleon structure known as the Chiral Bag Model [10], where the valence quarks are confined in a small core. It has been further shown that the baryonic charges of the valence quarks inside the core are screened due to the polarization of the Dirac sea, but together with the baryonic charge outside $r_{\rm c} < r \lesssim r_{\rm B}$, the total baryonic charge indeed adds up to 1. Furthermore, because $\zeta(r)$ is zero in the region $0 \le r \le r_{\rm c}$, the quarks are massless here and chiral symmetry is restored and we have, a phase transition from the $\zeta = f_\pi$ region ($r_{\rm c} < r \lesssim r_{\rm B}$), where chiral symmetry is spontaneously broken. We note that the Chiral Bag Model with a small core containing valence quarks provides the same results for the low energy properties of the nucleon as the topological soliton model [10]. In particular, the size of the baryonic charge density in the Chiral Bag Model will be $r_{\rm B} \simeq 0.5$ F as in the topological soliton model. We now face a new question: What is the behavior of the scalar field $\zeta(r)$ for large r beyond $r_{\rm B}$?

Our phenomenological investigation of high energy pp and $\bar{\rm p}$p elastic scattering has shown that protons and antiprotons have outer hadronic clouds. In pp and $\bar{\rm p}$p forward elastic scattering, the outer cloud of one proton interacts with that of the other proton or antiproton giving rise to diffraction scattering. Such an outer cloud can be envisioned by considering a behavior of the scalar field $\zeta(r)$ beyond $\zeta(r) = f_\pi$ ($r > r_{\rm B}$) region as shown in Fig. 2. The scalar field, being non-vanishing in the quark-scalar sector (Eq. (19)), interacts with the quarks and antiquarks making them massive. This lowers the energy of the ground state, which is now an interacting Dirac sea. This phenomenon is analogous to superconductivity. We have a condensed q$\bar{\rm q}$ ground state surrounding the topological baryonic charge. This provides the outer

hadronic cloud of a proton or antiproton, and we are led to the physical structure of the proton as shown in Fig. 1 — a Condensate Enclosed Chiral Bag.

5. Elastic Scattering Processes

The proton structure that has emerged from our effective field theory consideration (Fig.1) leads to three main processes in elastic scattering (Fig. 3): i) In the small $|t|$ region, i.e. in the near forward direction, as we have mentioned above, the outer cloud of $q\bar{q}$ condensate of one proton interacts with that of the other giving rise to diffraction scattering. This process underlies the observed increase of the total cross section with energy and the equality of pp and $\bar{p}p$ total cross sections at high energy. ii) In the intermediate momentum transfer region ($|t| \simeq 1 - 7$ GeV^2), the topological baryonic charge of one proton probes that of the other via vector meson ω exchange. This process is analogous to one electric charge probing another via photon exchange. The spin-1 ω acts like a photon – because of its coupling with the topological baryonic charge. iii) In the large $|t|$ region: $|t| \gtrsim 7$GeV^2, one proton probes the other at transverse distances less than 0.1 fm. Elastic scattering in this region is viewed in our model as a hard collision of a valence quark from one proton with a valence quark from the other as shown in Fig. 4. We refer to elastic scattering with such large $|t|$ as deep-elastic scattering. For deep-elastic scattering, we have considered two QCD processes. The first involves the exchange of reggeized gluon ladders (a BFKL ladder) plus next-to-leading order corrections (also referred to as hard pomeron). The other QCD process we have considered is where the low-x gluon cloud of a valence quark in one proton interacts with that of a valence quark in the other proton [11].

6. Quantitative Results

Our predicted pp elastic $d\sigma/dt$ at c.m. energy 7 TeV due to the combined three processes – diffraction, ω-exchange and valence quark-quark scattering (from low-x qq interaction) is shown in Fig. 5. Also shown are separate $d\sigma/dt$ due to diffraction (dotted curve), ω-exchange (dot-dashed curve), and valence quark-quark scattering (dashed curve).
At $\sqrt{s} = 7$ TeV, we obtain $\sigma_{\rm tot} = 97.5$ mb, $\sigma_{\rm el} = 19.8$ mb, $\rho(t = 0) = 0.127$, $B(t = 0)$(nuclear) $= 27.77$ GeV^{-2}, $d\sigma/dt\,(t = 0) = 493.4$ mb/GeV^2.

Finally, in Fig. 6 our predicted elastic $d\sigma/dt$ at $\sqrt{s} = 7$ TeV with quark-quark scattering due to low-x gluons (solid curve) and due to hard pomeron (dashed curve) are shown and compared with the predicted $d\sigma/dt$ of Block et al. [12] and Bourrely et al. [13]. A distinctive feature of our predicted $d\sigma/dt$ is that the differential cross section falls off smoothly beyond the shoulder at $|t| \simeq 0.5$ GeV^2, while the Block et al. and Bourrely et al. models predict visible oscillations in $d\sigma/dt$.

7. Concluding Remarks

i) We find that the topological soliton model of the nucleon provides an appropriate backdrop for the proton structure that we have arrived at.

ii) The large mass problem of the topological soliton model is resolved by realizing that, if the scalar field falls sharply from $\zeta(r) = f_\pi$ to $\zeta(r) = 0$ – somewhat like $\zeta(r) = f_\pi\, \theta(r - r_c)$, then the mass of the soliton decreases by a significant amount. This also means the model becomes essentially a Chiral Bag model.

iii) In the region beyond the topological baryonic charge density ($r > r_B$), the scalar field decreases smoothly (Fig. 2), its nonvanishing value makes the quarks and antiquarks massive, lowers the energy of the Dirac sea, and we have a $q\bar{q}$ condensed ground state forming an outer cloud of the proton. This leads to the structure of the proton shown in Fig. 1.

iv) Our quantitative $d\sigma/dt$ calculations at 7 TeV show that there are three distinct processes which come to play. For small $|t|$ - it is diffraction, for intermediate $|t|$ ($1\ \text{GeV}^2 < |t| < 7\ \text{GeV}^2$) - it is ω-exchange probing baryonic charge densities of the colliding protons, and for large $|t|$ ($|t| > 7\ \text{GeV}^2$) - it is valence quark-quark scattering via gluon ladders or low-x gluon-gluon cloud interaction.

v) Our predicted $d\sigma/dt$ decreases smoothly from $|t| \approx 1\ \text{GeV}^2$ to $|t| = 10\ \text{GeV}^2$, while $d\sigma/dt$ predicted by Block et al. model and Bourrely et al. model show visible oscillations.

P.S. The TOTEM Collaboration has now published their elastic $d\sigma/dt$ measurement at $\sqrt{s} = 7$ TeV in the momentum transfer range $0.36 < |t| < 2.5\ \text{GeV}^2$: The TOTEM Collaboration et al., EPL (Europhysics Letters) **95** (2011) 41001. The Collaboration has also published most recently their first measurement of the total proton-proton cross section at 7 TeV: The TOTEM Collaboration et al., EPL **96** (2011) 21002. Their results are: $\sigma_{tot} = 98.3 \pm 3$ mb, $\sigma_{el} = 24.8 \pm 1.4$ mb, $B = 20.1 \pm 0.5\ \text{GeV}^{-2}$ (from exponential fit).

8. References

[1] M. M. Islam, J. Kašpar, R. J. Luddy, A. V. Prokudin, *CERN Courier*, December 2009, p.35.

[2] A. Hosaka and H. Toki, Quarks, Baryons and Chiral Symmetry (World Scientific), 2001.

[3] M. Bando, T. Kugo, S. Uehara, K. Yamawaki and T. Yanagida, *Phys.Rev.Lett.* **54** (1985) 1215.

[4] U. G. Meissner, N. Kaiser, A. Wirzba and W. Weise, *Phys.Rev.Lett.***57** (1986) 1676.

[5] R. K. Bhaduri, *Models of the Nucleon: From Quarks to Soliton*, (Addison-Wesley, 1988), Ch.7.

[6] M. M. Islam, R. J. Luddy and A. V. Prokudin, *Int. J. Mod. Phys*. **A21** (2006) 1-41.

[7] U. G. Meissner, N. Kaiser and W. Weise, *Nucl. Phys.* **A466** (1987) 685.

[8] M. M. Islam, *Z. Phys.* **C53** (1992) 253.

[9] L. Zhang and N. C. Mukhopadhyay, *Phys. Rev.* **D50** (1994) 4668.

[10] A. Hosaka and H. Toki, *Phys. Rep.* **277** (1996) 65.

[11] For details, see M. M. Islam, J. Kašpar, R. J. Luddy and A. V. Prokudin, *Proceedings of the 13th Int. Conf. on Elastic and Diffractive Scattering* (EDS 2009, CERN), edited by M. Deile, D. d'Enterria and A. De Roeck, p.48.

[12] M. M. Block, E. M. Gregores, F. Halzen and G. Pancheri, *Phys. Rev*. **D60** (1999) 054024.

[13] C. Bourrely, J. Soffer and T.T. Wu, *Eur. Phys. J.* **C28** (2003) 97.

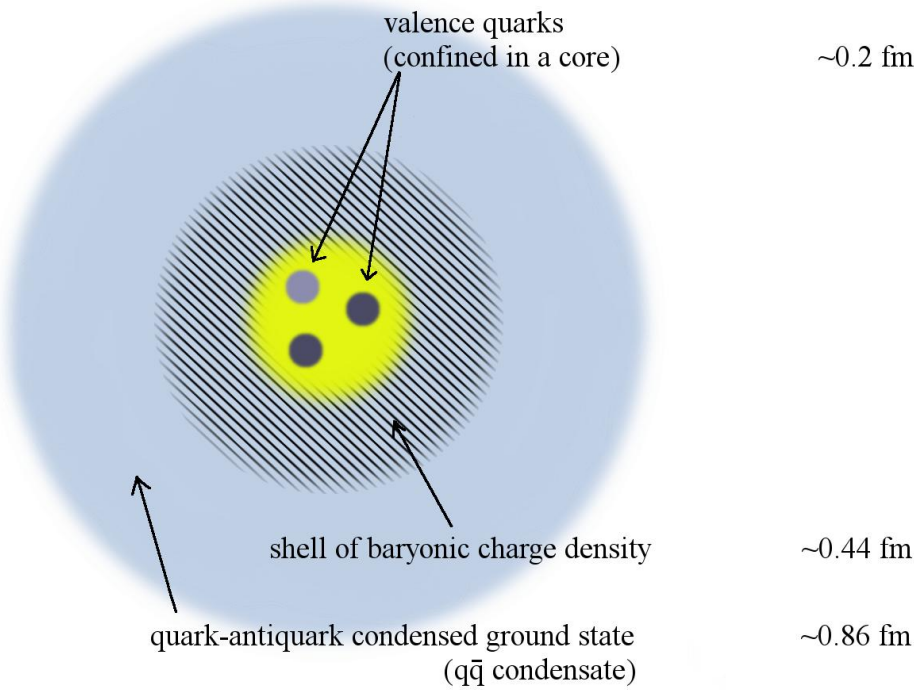

Fig. 1. Physical picture of the proton as a Condensate Enclosed Chiral Bag.

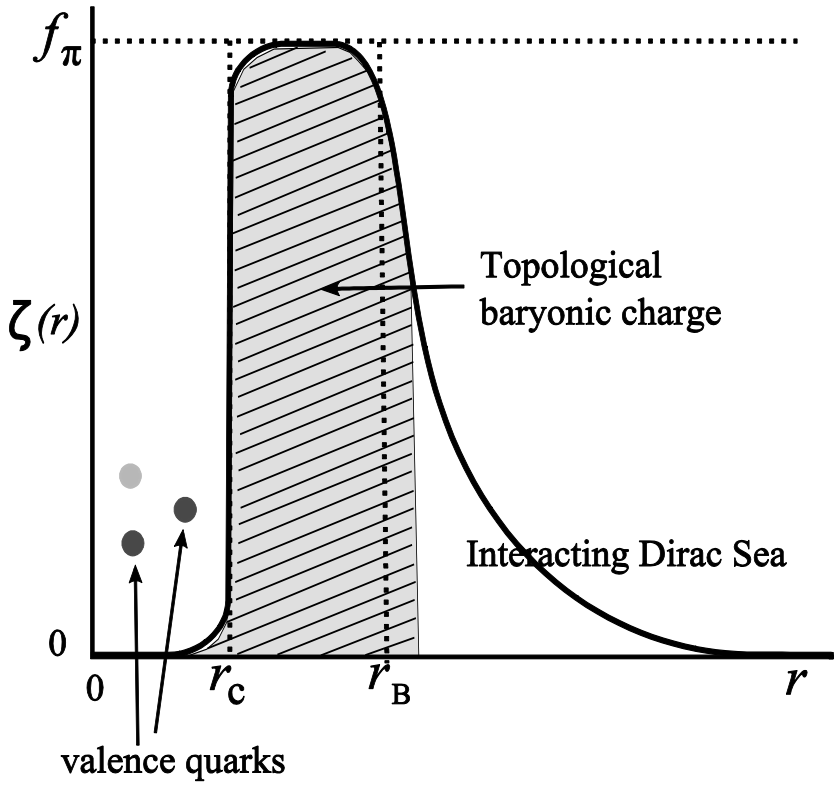

Fig. 2. Scalar field $\zeta(r)$ as a function of r.

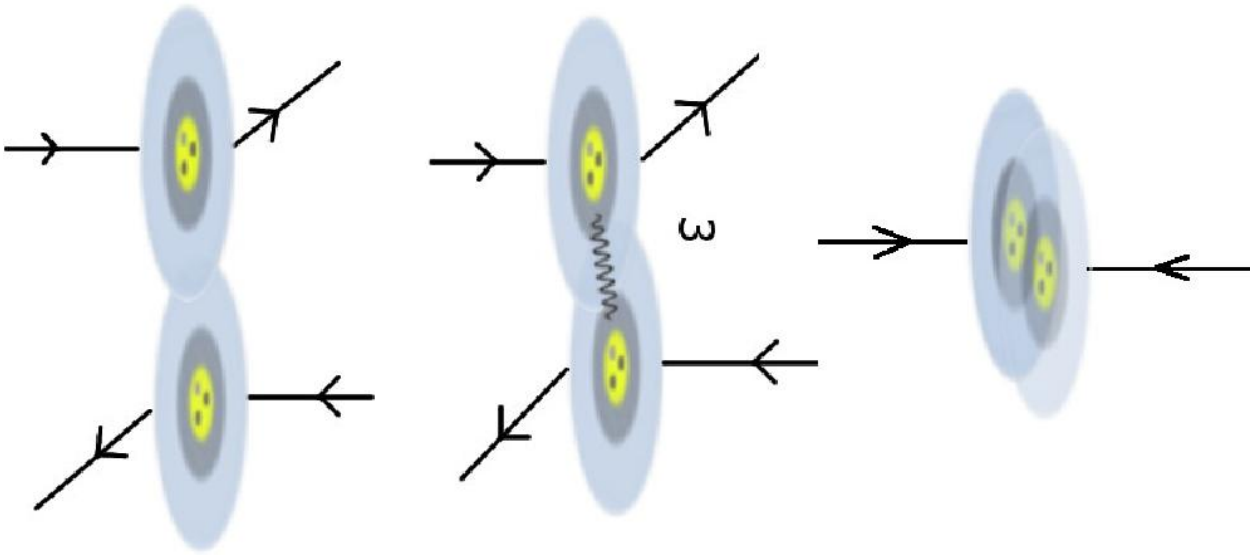

Fig. 3. Elastic scattering processes (from left to right):
1) diffraction, 2) ω-exchange, 3) short-distance collision ($b \lesssim 0.1$ fm).

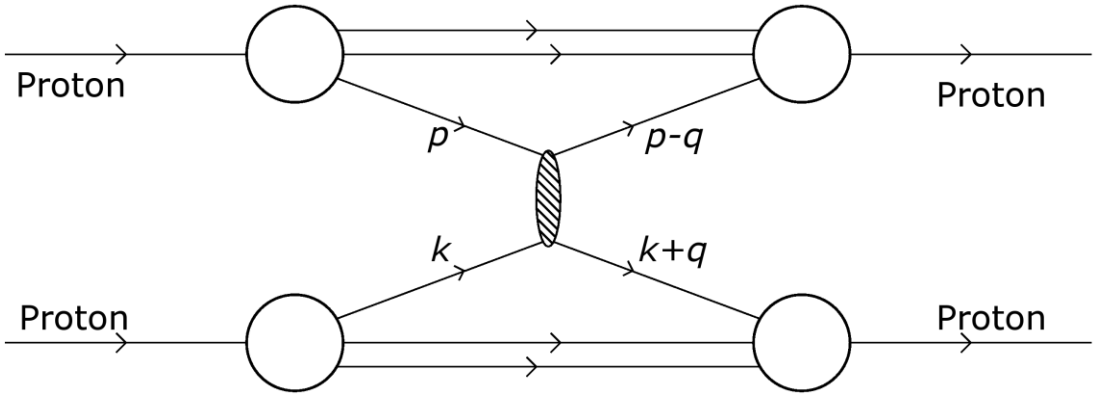

Fig. 4. Hard collision of a valence quark of 4-momentum p from one proton with a valence quark of 4-momentum k from the other proton, where the collision carries off the whole momentum transfer q.

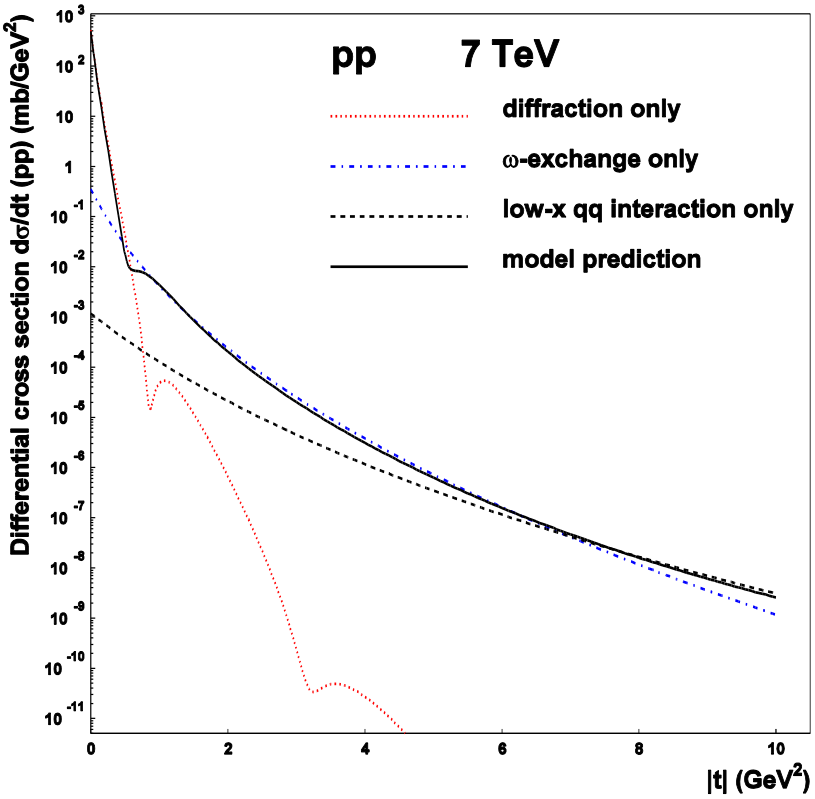

Fig. 5. Our $d\sigma/dt$ prediction at 7 TeV.

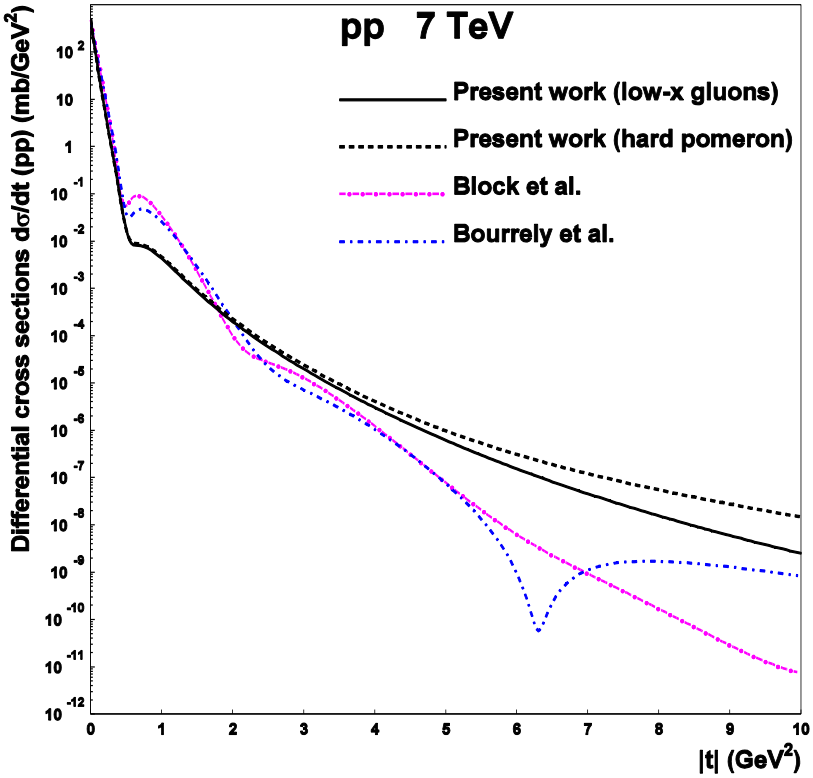

Fig. 6. Our $d\sigma/dt$ predictions at 7 TeV compared with the $d\sigma/dt$ predictions of Block et al. and Bourrely et al.